Food and Bioprocess Technology
https://doi.org/10.1007/s11947-022-02953-7

RESEARCH

Evaluating an Ultrasonic Magnetostrictive Transducer with Conical Nickel Core: Performance and Application

Danial Gandomzadeh[4] · Mohammad Hossein Abbaspour-Fard[1] · Abbas Rohani[5] · Yeganeh Sabeghi[2] · Soheil Movahed Fakhr[3]

Received: 29 August 2022 / Accepted: 20 November 2022

Abstract

In recent years, ultrasonic machining has been developing rapidly, and it is used in areas such as abrasive machining, cleaning, and welding. In this research, a magnetostrictive device with pure nickel conical core with cone angle of 30° was constructed. The observed sound pressure level was used as a measure of transducer performance. Also, the ability of the device to reduce the residual pesticide on cucumber surface due to cavitation was evaluated. The results showed that the sound pressure from simulation by JMAG-Designer software is almost the same as the sound pressure produced in the constructed transducer. To assess the performance of the device in removing residual pesticide from cucumber surface and evaluate the changes in peel texture of cucumber, the gas chromatography (GC) and scanning electron microscope (SEM) methods were used, respectively. The GC results showed that with 20 min treatment, the removal of pesticide based on height and chromatogram area was 75% and 83%, respectively. The SEM results showed that by increasing the treatment time, the stomatal pore area reduced from 144.74 μm^2 (reference) to 30.56 μm^2 (20 min treatment). These results are promising; hence, further research is suggested towards enhancing the device for commercial use in biomaterials processing operations such as cleaning and removing pesticides from fruits and vegetables.

Keywords Magnetostrictive ultrasonic transducer · Residual pesticide · Cleaning · GC · SEM

Introduction

In recent years, ultrasonic machining has developed rapidly. It has been used in applications such as ultrasonic abrasive machining, cleaning, and welding. Fruits and vegetables contain important nutrients that are essential for human health. But agricultural pesticides are widely used to protect products against insects, diseases, and maximizing crop yields. Residual pesticides have been considered in terms of their effects on human health as well as environmental effects because these pesticides cause diseases such as cancer and reproductive endocrine disorders (Mac Loughlin et al., 2018).

In general, different methods are used for peeling and cleaning agricultural products including manual, mechanical, chemical, enzymatic, and thermal (Tapia et al., 2015). Conventional, mechanical, and chemical methods and immersion in hot water cause adverse effects on the product (Wang et al., 2016). Alkaline solution or steam pressure can also be used for this purpose.

✉ Mohammad Hossein Abbaspour-Fard
abaspour@um.ac.ir

Danial Gandomzadeh
da.gandomzadeh@stu.um.ac.ir

Abbas Rohani
arohani@um.ac.ir

Yeganeh Sabeghi
ye.sabeghi@stu.um.ac.ir

Soheil Movahed Fakhr
smovahedfakhr@hotmail.com

[1] Faculty of Agriculture, Ferdowsi University of Mashhad, University Campus, Azadi Square, Mashhad, Iran

[2] Department of Food Science and Technology, Faculty of Agriculture, Ferdowsi University of Mashhad, Mashhad, Iran

[3] Department of Electronics Engineering, Faculty of Electrical Engineering, Montazeri Technical College of Mashhad, Mashhad, Iran

[4] Department of Biosystems Engineering, Faculty of Agriculture, Ferdowsi University of Mashhad, Mashhad, Iran

[5] Faculty of Agriculture, Ferdowsi University of Mashhad, Mashhad, Iran

Published online: 28 December 2022

However, these methods have some disadvantages such as excessive water and chemical consumptions, high cost, as well as problems related to peeling waste (Pan et al., 2015). In addition, infrared (IR) (Li & Pan, 2014) and ultraviolet (UV) radiations (Ignat et al., 2015; Xu & Wu, 2014) can be used for peeling and cleaning agricultural products. Chemical methods use natural acids such as aceticacid, benzoicacid, citricacid, malicacid, sorbicacid, succinicacid, and tartaricacid (Tapia et al., 2015) as well as antimicrobial agents such as peroxyacetic acid, chlorine dioxide, ozone, electrolyzed water, chlorine (Doménech et al., 2013), and Essential Organic Oils (EOS) (Zhang et al., 2014). These compounds, have some benefits such as antiseptic properties and reasonable price but raise concerns about the reaction of chlorine with organic matter and toxic properties (Maffei et al., 2016). Alternative methods such as ultrasound can be used to remove residual chemicals from agricultural products with high performance (Lozowicka et al., 2016). Piezoelectric ultrasound transducers have been used for this purpose, but to amplify the amplitude of the generated waves, a horn, which causes power loss, must be used (Fang et al., 2018). In other words, due to the heating and low thermal conductivity of piezoelectric materials, it is necessary to use water as a coolant. But the use of cooling water increases the size of the ultrasonic transducer. Therefore, silicon layers can be used to focus ultrasound waves in a wide bandwidth. These silicone layers also provide the possibility of heat transfer (Chang et al., 2014) because the production of flat piezoelectric ceramics is economical and the sound fields can be concentrated with the help of acoustic lenses (Thomas et al., 2018). For this purpose, different materials can be used, such as composite polymers, which include metal powders and epoxy. Although these lenses improve the efficiency of piezoelectric transducers, but as a problem, these lenses can only be used in special transducers (Sun et al., 2023). Magnetostrictive materials are good alternatives to convert electrical energy to ultrasound and used in various fields such as cleaning (Grange & Brown, 1969), sonochemistry, industrial processes, and medicine because they have high energy density and high response speed (Cai et al., 2016). In order to optimize the design of these transducers at a lower cost, their performance should be examined in software environments with applied effective parameters. These parameters included the number of coil turns, electrical frequency, permanent magnets position, and core geometry. In fact, the fluctuations of magnetostrictive force in the longitudinal direction of the transducer are very important in the generation of ultrasonic waves. It has been shown that conical cores with an angle of 30° are able to generate the maximum fluctuations along the longitudinal axis (Gandomzadeh & Abbaspour-Fard, 2020).

The contamination level of products should be controlled in order to assure consumer health, improve the management of agricultural resources, and prevent economic losses. This evaluation is performed by the MRL (maximum residue limits) index. This parameter actually determines the maximum allowable concentration of residual pesticides inside or outside food products in terms of μg/kg (Mac Loughlin et al., 2018). Many methods are used to detect residual pesticides on agricultural products. These methods include gas chromatography (GC), high-performance liquid chromatography (HPLC), HPLC/GC, mass spectra (MS) (Jiang et al., 2019), and enzyme-linked immunoassay (ELISA), GC–MS, liquid chromatography/mass spectra (LC–MS), and quadrupole time-of-flight mass spectrometry (Q-TOF MS) (Xiu-ping et al., 2017). In order to evaluate changes in the surface quality of biological materials due to ultrasonic application, a wide range of special tools and equipment are required. One of these common methods is the scanning electron microscope (SEM).

Fresh fruit and vegetables must be safe against microbiology contamination and chemical content as they are generally consumed raw. As US processing has been reported to be a potential alternative to chlorine in disinfection steps, studies have been and must be further carried out in order to better understand the outcomes. The most common applications are shown in Table 1. The utilized frequencies were 20, 30, 35, 40, and 135 kHz. Treatment times ranged from 2 s to 60 min. In addition, several organic materials have been evaluated. These include process water, juice "tomato, fruit, and orange," fresh-sliced "button mushrooms and coconut," meat "raw poultry," and whole "watercress, calçots, and cucumber." According to Table 1, most of these studies are related to piezo ultrasonic transducer, and few studies have been conducted on magnetostrictive ultrasonic transducers with pure nickel core. Also, previous studies have investigated other parameters such as disinfection, microbial inactivation, microorganism inactivation, and improving safety and quality. The results of these studies showed that, in addition to improving the quality and appearance of foods and vegetables, ultrasound is capable of decreasing microbial loads and microorganisms of organic materials. However, in the current research, not only the safety and quality parameters of the cucumber was considered, but also the performance parameters of the magnetostrictive transducer were studied.

In this study, the ability of a magnetostrictive transducer equipped with a conical core, made of pure nickel in generating ultrasonic wave, to create turbulence in liquid for cleaning fruits and vegetables was evaluated. Due to the limitations of the existing load cells in measuring high-frequency forces, the performance of this transducer was evaluated by measuring its created sound pressure, using a decibel meter. The decibel meter data were then compared with the results of numerical simulation using the JMAG-Designer software. In addition, the performance of the device in creating cavitation to disperse waterproof paints in aqueous solvents was investigated by image processing. On the other hand, cucumber is one of the most widely consumed products among fruits and vegetables, widely used in salads and cold soups. Few studies have been performed on the effect

Table 1 Effect of ultrasonic treatment solely or in combination with other methods

Organic material	Treatment	Freq. (kHz)	Purpose	Time	Results	Ref
Process water	High-power ultrasound (HPU)	20	Disinfecting and recycling (E. coli O157:H7)	60 min	The higher the power density and temperature, the higher the efficiency. Agglomerates >90 µm were reduced to only 11% by HPU	(Gómez-López et al., 2014)
Tomato juice	Thermosonication	35 or 130	Microbial inactivation	5 min	Thermosonication allowed increased retention of color attributes as well as polyphenol, lycopene, anthocyanin, and antioxidant capacity retention	(Lafarga et al., 2018)
Fruit juices	High-intensity ultrasound (USc) and/or UV-C	20	Microorganisms inactivation	Up to 20 min	Its efficiency is limited to clear	(Char et al., 2010)
Orange juice	Thermosonication and pulsed electric fields	30	Inactivation the Staphylococcus aureus	10 min	TS/PEF did not affect the pH, conductivity, or Brix and had a milder impact on the juice color than thermal treatment	(Walkling-Ribeiro et al., 2008)
Fresh-sliced button mushrooms	Acidic electrolyzed water and ultrasound (LcEW + US)	40	Evaluating the microbial loads	3 min	Significantly inhibited the activities of polyphenol oxidase (PPO) and peroxidase (POD) and controlled the counts of total bacteria (TBC)	(Wu et al., 2017)
Fresh-cut coconut	High-power ultrasound-assisted carbon dioxide	30	Inactivation kinetics of both the natural microbiota and Salmonella	2 min	HPCD + HPU increased microbial inactivation rates compared with HPCD alone	(Ferrentino et al., 2015)
Raw poultry	High-intensity ultrasound	40	Reducing numbers of Campylobacter	16 min	No viable Campylobacter were detected	(Haughton et al., 2010)
Watercress	Thermosonication	20	Better quality	0.03 and 0.5 min	The improvement of the blanched watercress quality	(Cruz et al., 2009)
Calçots (*Allium cepa L.*)	Ultrasound (US)	40	The physical and microbiological quality	0, 10, 25, and 45 min	A decrease of 1-log reduction was observed after treating for 45 min	(Zudaire et al., 2018)
Whole tomato	Water heat treatment, ultrasounds, thermosonication, and UV-C radiation	45	Improving safety and quality	30 min	WHT, TS, and UV-C proved to be more efficient in minimizing color and texture changes with the additional advantage of microbial load reduction	(Pinheiro et al., 2016)
Whole cucumber	Ultrasonic (magnetostrictive transducer)	20	Removing residual pesticide and evaluating the changes in peel texture as the quality parameter	0, 5, 10, and 20 min	The removal of pesticide was 83%. By increasing the treatment time, the stomatal pore area reduced	***This work***

of ultrasonic treatment time on cucumber washing. In this study, the amount of residual pesticide on cucumber and also the textural changes in its peel after ultrasonic treatment were investigated by GC and SEM methods, respectively because these changes affect the digestibility of cucumber peel and also its shelf life.

Materials and Methods

Manufacturing the Mechanical Parts of Ultrasonic Transducer

Nickel plates with 99.99% purity (Vale Inco, Canada) were purchased and used to make the magnetostrictive core. Pure metals have high melting temperatures which is 1455 °C for nickel (Smithells, 1976). By some modifications on the existing induction furnace (Ferdowsi University of Mashhad, Nano Laboratory), the pure nickel was cast in the prepared mold. After casting the pure nickel in the induction furnace, the cast specimen was machined to achieve the desired dimensions of the core. The housing and cap of the device were made of 316-L austenitic stainless steel. Among the characteristics of this steel are high resistance to corrosion, higher strength in high temperatures, good forming ability, and high tolerance to stress (AZoM, 2004). The housing and its cap are responsible for compressing the inside components of transducer (core and winding). According to Fig. 1, in order to tighten the housing cap and compress the internal parts of the transducer, a head was built on the top of the cap. As shown in this figure, polyethylene material was used to make the coil spool of device. The thickness of this spool was considered to be 5 mm to ensure enough mechanical strength in the coil during the winding process and also when applying high electrical power (due to relatively high heat) to the coil.

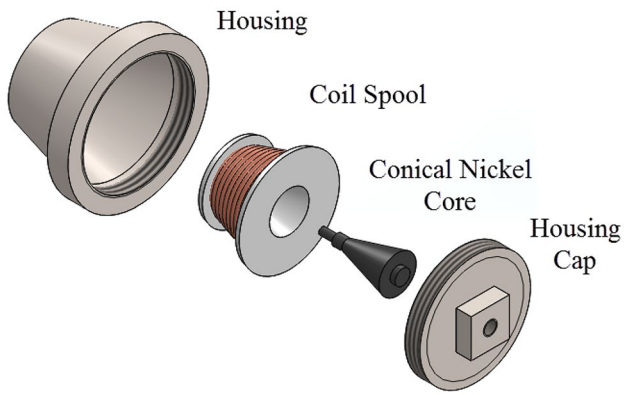

Fig. 1 The exploded view of magnetostrictive ultrasonic transducer

Electrical Specifications of Coil and Driver Circuit

The operating frequency of the magnetostrictive ultrasonic transducer was set to 20 kHz (Gandomzadeh & Abbaspour-Fard, 2020). In this study, the inductance of the coil was compared in two different modes. Because at high frequencies, based on the skin effect, the current through the coil tends to move away from the center of the wire. Therefore, the number of parallel strands of wire should be increased as much as possible in order to increase the cross section to pass high-frequency current (Bartoli et al., 1996). For this purpose, a bundle of 100-strand wire with a length of 10 m was prepared (known as Litz wire). The Litz wire consisted of 0.2 wires. Then the coil was wound with the same number of turns by ordinary wire and Litz wire and the results were compared. While winding the wires, insulation paper (Presspahn Limited) and air drying varnish were used to create electrical insulation and eliminate the vibrations of the wires, respectively.

In pure induction circuits, the source power is used to create a magnetic field. Also in RLC circuits, if resistive, inductive, and capacitive loads are in series, the resonance frequency (f_r) is achieved when the magnetic resistance of the inductor load is equal to the capacitive resistance of the capacitive load. These circuits are called series resonant circuits. For this purpose and as seen in Fig. 2, the driver circuit designed by Mahbodtronics Company, Iran. This circuit has a half bridge consisting of two IGBTs and also a capacitive bank which was placed in series with the magnetostrictive transducer coil. The features of this circuit include switching high currents (more than 30 amps) with high operating frequency (more than 100 kHz). The driver is powered by a 12-V power supply to switch IGBTs and supply the required voltage to the microcontroller and the other electronic components via an LM7805 regulator. Also, a variable transformer was used to provide the required power of the magnetostrictive transducer. The operating frequency of the driver is adjusted by an ATMega8 microcontroller. As previously stated, given that the operation frequency of the transducer was considered equal to 20 kHz and the circuit inductance was equal to 74 μH, the capacitor bank capacitance was calculated equal to 1 μF, because the resonant frequency of the driver circuit must be close to the desired operating frequency. However, due to the fact that the required current of the transducer is infinite in the resonant frequency, the operating frequency of the microcontroller should be shifted as much as 10 to 20% to the inductive area. Therefore, by using the capacitor bank, the resonant frequency of the driver circuit was adjusted to approximately 18 kHz, and to move away from the resonance zone, the operating frequency of the microcontroller, which is the operating frequency of the transducer, was set at 20 kHz.

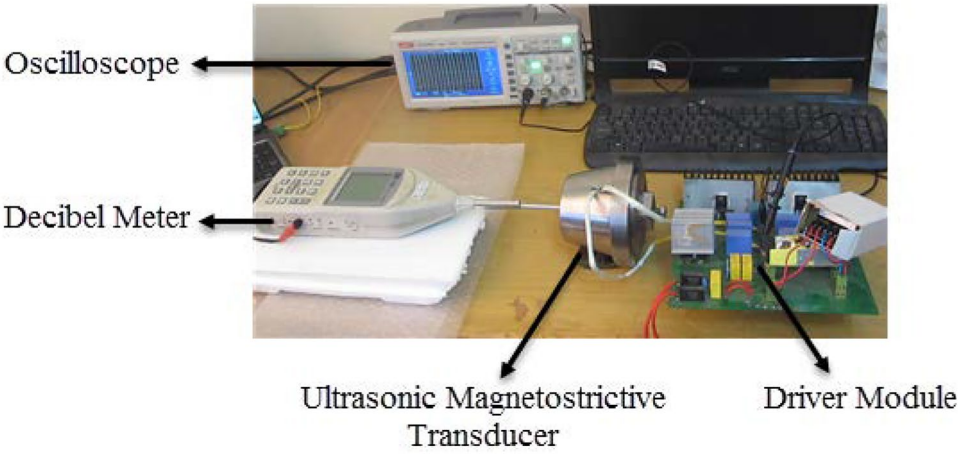

Fig. 2 Sound pressure measurement setup including the driver circuit and measuring devices

Sound Pressure Measurement

In magnetostrictive transducers, the fluctuations of the magnetostrictive force along the longitudinal axis are the key parameters affecting the cavitation phenomenon. Also according to the Nyquist law, the sampling rate of the generated ultrasound must be at least twice the operating frequency (Wang et al., 2021). Due to the high operating frequency in this study (20 kHz) on the other hand, low sampling rate of the existing load cells, it was not possible to directly measure the magnetostrictive force. So, the performance of the transducer was evaluated as its sound created, and the sound pressure measured from the real transducer was compared with the simulation model. So, according to Fig. 2, the ultrasonic generated by the device was measured by a decibel meter (TES-1358). The decibel meter was placed horizontally in front of the device. In this study, the dimensions of the transducer components, including the core, spool, coil, and shell, were considered in the simulation according to the real sample. As shown in Fig. 3, the large diameter of the conical core (D), the small diameter of the conical core (d), and its length (L) are 37, 1, and 50 mm, respectively. The simulation of the transducer was carried out in the JMAG-Designer software environment, and the electrical parameters that cause the excitation of the transducer were selected according to Table 2.

The electrical parameters of the transducer were measured using a multimeter, clamp ammeter, and oscilloscope which are given in Table 2. The decibel value was measured in two different modes, i.e., when the driver circuit is turned off (solely surrounding sound with no sound from transducer) and when the magnetostrictive transducer is on (surrounding sound + transducer sound). The sound level in the first and second mode was 35.6 and 66.5 dB, respectively. In other words, by turning on the driver circuit, the decibel increased by 30.9 dB.

Simulation in JMAG-Designer Software

The effects of different parameters on the performance of the magnetostrictive transducer were investigated performing the simulation runs in the 3D environment of JMAG-Designer 16.0 software. This simulation software is used for electrical, electromagnetic, mechanical, and thermal analysis of electrical equipment. The analysis of this software is based on the so-called finite element method (FEM)

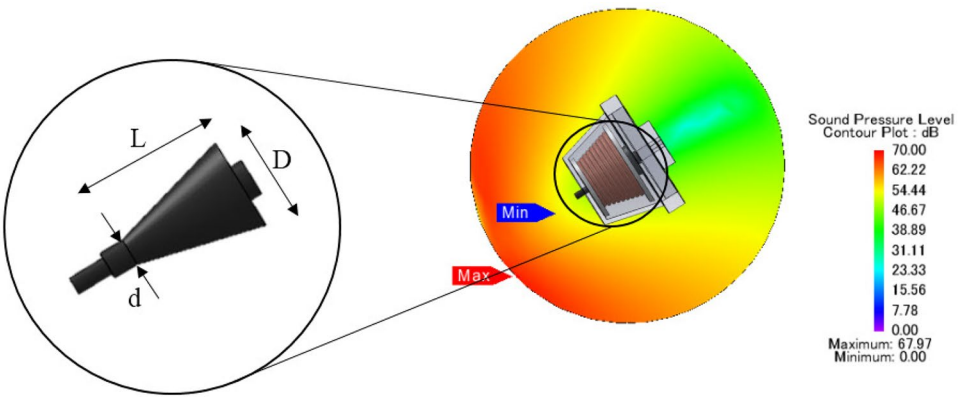

Fig. 3 The generated sound pressure level on a spherical shell with a diameter of 100 mm in the simulation model

Table 2 Electrical specifications of coil used in the magnetostrictive transducer

Wire Specification		Coil Specification	
Wire Strands No.	100	Frequency	20 kHz
Wire Diameter/Gauge	32/0.2 mm	Current	5 A
Wire Resistance	1.7 Ω	Voltage	78 V
Inductance	74 μH		

(Apostoaia, 2013). This transducer was analyzed by transient analysis method in JMAG-Designer software environment. In this analysis, magnetostriction and FEM coil conditions were applied to a nickel core containing a copper coil, respectively. The electrical circuit consisted of a current source and a coil. The boundary conditions used in this study were symmetry boundary and natural boundary. The former was applied to the surfaces, which are parallel to the magnetic flux, and the latter was applied to surfaces perpendicular to the magnetic flux. Moreover, in the mesh settings procedure, the basic settings were done by standard meshing method, based on the recommendations provided in the software instruction. In addition, the size of the elements in the element size section was selected automatically (Gandomzadeh et al., 2022). Then the sound pressure level was applied on the transducer as a model condition. The sound pressure was calculated on a spherical shell with a diameter of 100 mm.

Image Processing Procedure to Evaluate the Dispersion Effect of Transducer

In order to evaluate the performance of the device, a waterproof paint dispersion test was used. In this test, the dispersion rate of waterproof paint in water was evaluated. Image processing is a technique to monitor various processes, including monitoring the ripening of agricultural products such as mango, banana, and apple in the ripening room to achieve the desired conditions (Eyarkai Nambi et al., 2016). In this test, a drop of waterproof paint was poured at the bottom of a 50-cc glass bottle, and subsequently, by turning on the ultrasonic transducer, the paint dispersion process in aqueous solvent was filmed. In order to evaluate the dispersion effect of the transducer by image processing, color snapshots were captured after 10, 20, 30, 40, 50, and 60 s (0.16, 0.33, 0.5, 0.66, 0.83, and 1 min), since the paint dispersion was negligible before 10 s (0.16 min). Red, green, and blue channels of the images were extracted using MATLAB software. Histogram adjustment was used to create more distinction between the background and the paint dispersed in the water. In other words, multiplication operations were used to increase color intensity (Łoza et al., 2013). After reading the images in MATLAB software environment, a suitable coefficient was selected to increase the color intensity by trial and error method, and this coefficient was applied to color images and the extracted channels.

Cucumber Sampling

The use of methods such as washing, peeling, blanching, smoking, frying, boiling, and canning showed that the residual levels of pesticides decreased from 0.80 to 0.10 μg/kg. On the other hand, the use of some combined methods such as ultrasound and low-intensity electric currents reduces potato fungicides by 95.1% (Azam et al., 2020). In order to ensure the concentration of residual pesticides on the crop, cucumbers prepared from a local greenhouse located in Fariman city, where biological pesticides were used to grow this product. The variety of these cucumbers was DIVA. Their average physical dimensions, which include diameter, length, and mass, were 14.1 and 27.3 mm, and 70.8 gr, respectively. In this study, Diazinon pesticide was used to investigate the effects of ultrasonic treatment on reducing the residual pesticides on cucumber samples. This pesticide that is frequently used against insects on fruits and vegetables such as cucumbers, tobacco, forage, as well as soil nematodes. It is also used to protect greenhouses and mushroom farms from winged insects. In addition, Diazinon is one of the organophosphorus pesticides that affects human health and is easily absorbed through the gastrointestinal tract, skin, and respiratory tract (Cengiz et al., 2006). The chemical formulation of this pesticide is $C_{12}H_{21}N_2O_3PS$. Based on the application, this pesticide can be used from 1.12 to 8.97 kg per hectare, but for this purpose, considering the concentration of 2 ml/L (Cengiz et al., 2006), the solution of Diazinon was spread evenly on the samples. The solution was sprayed by a hand sprayer with a tank capacity of 70 ml.

Ultrasonic Treatment

Since this transducer is equipped with a nickel core with low magnetostriction effects, its ultrasonic output power is low. For this purpose, in order to increase the effect of ultrasound waves on cucumber samples, a 250-ml lab beaker was used to place two cucumbers with the ultrasonic horn. In other words, the cucumber samples and transducer horn were immersed in the water of the beaker. Then, each sample was treated separately by ultrasound. The ultrasonic treatment time was variable and equal to 5, 10, and 20 min (Liang et al., 2012). However, due to the fact that more than 50% of the input power of these transducers is converted to heat, the propagation time of ultrasonic waves was such that every 1 min of propagation, the power supply was cut off for 2 min. This time pattern was considered for cooling the nickel core and the Teflon coil spool.

Sample Preparation for GC

Gas chromatography was used to evaluate the changes in the amount of residual pesticide on cucumber samples. To perform this test, four samples including reference, 5 min, 10 min, and 20 min treatments were selected. Each sample was first crushed separately in a blender at 9000 rpm for 5 min and then placed in a variable-speed homogenizer. However, in order to ensure that all the cucumber pulps were crushed and prevent remaining pulps between the homogenizer blades, the blended samples were first completely crushed in a laboratory mortar and passed through filter paper. In the homogenizer, the samples were completely uniform for 2 min at variable speeds. The homogenized samples were transferred separately to the GC laboratory of Ferdowsi University of Mashhad in glass containers. Samples were evaluated by QuEChERS method (Koesukwiwat et al., 2010).

Sampling for SEM

SEM images were used to investigate the textural changes of cucumber peel caused by the application of ultrasonic waves. To perform this test, four samples including reference, 5 min, 10 min, and 20 min treatments were selected. Samples were prepared biologically (Smith & Fleming, 1979), and then SEM images were taken in Central Laboratory of Ferdowsi University of Mashhad.

Results and Discussion

Sound pressure level was used as a measure of transducer performance. The performance of transducer was also investigated as its ability to disperse waterproof paints in aqueous solvents by image processing. Then Diazinon pesticide, which is widely used in agricultural applications including the production of cucumber, was used. After spreading Diazinon pesticide solution on cucumber products, ultrasonic treatment was applied on the samples for 5, 10, and 20 min. To determine the residual pesticide and evaluate the peel texture of cucumber product, the GC and SEM methods were used respectively.

Sound Pressure Level Test

As previously stated, in order to reduce heat loss and select a suitable conductor for applying the high-frequency current through the coil, the spool was wound by an ordinary wire and also Litz wire with the same number of coil turns. The purpose was to compare the performance of these two types of wirings. The results showed that the inductance of the coil with 100 turns for the coil with ordinary wire and Litz wire was 112.9 and 74 microhenry, respectively. Thus, by increasing the number of strands in the Litz wire, the resistance created at high frequencies decreases (Tourkhani & Viarouge, 2001).

In order to compare the real transducer with the simulation model, the sound pressure was measured. This parameter has been used to evaluate the performance of ultrasonic transducers (Ishiyama et al., 2003; Wang et al., 2006). The sound pressure produced is affected by the size of transducer. This increase is about 3 to 5 dB (Ishiyama et al., 2003). However, due to the small size of the transducer in this study, this effect can be ignored. Figure 3 shows the sound pressure distribution of the simulated transducer using the JMAG-Designer software. As mentioned, this 3D analysis was performed at a frequency of 20 kHz. The maximum point (red color) is located exactly in front of the transducer horn. But the minimum point (violet color) is located behind the image. The approximate position of this point was displayed by the software for the user on the spherical shell with a diameter of 100 mm. On the other hand, due to the high frequency, the position of the points changes in each snapshot. In this image, a moment of this analysis was shown.

In Fig. 4, the sound pressure level diagrams in three different modes are presented (simulated, real model, and ambient + real model). In other words, the decibel meter used in this test was able to measure the absolute decibel of the transducer and the decibel of the transducer along with the decibel of the ambient. Both were mentioned in the results. As seen the average sound pressure level in the simulated model, the absolute sound pressure level (solely from transducer) of the real transducer and the sound pressure level of real transducer with ambient sound were 33.98, 35.6, and 66.5 dB, respectively. A slight difference (4.5%) between the sound pressure level in the simulated model and the real transducer is seen. This is mainly due to the way of calculating the sound pressure. The sound pressure in the software environment was calculated on a spherical shell with a diameter of 100 mm, while in the real transducer, this was done by connecting the decibel meter directly in front of the core horn. Moreover, due to the mismatch of different properties of transducer in simulation and real model, some error is expected. Generally, in ultrasonic transducers, the transmitted power and sound pressure level increase with decreasing probe distance (Wygant et al., 2009).

Evaluating Dispersion Ability of the Magnetostrictive Device

By dropping the waterproof paint at the bottom of a glass bottle and applying the magnetostrictive transducer and filming the process, the color images and red, green, and blue channels were extracted in the MATLAB software

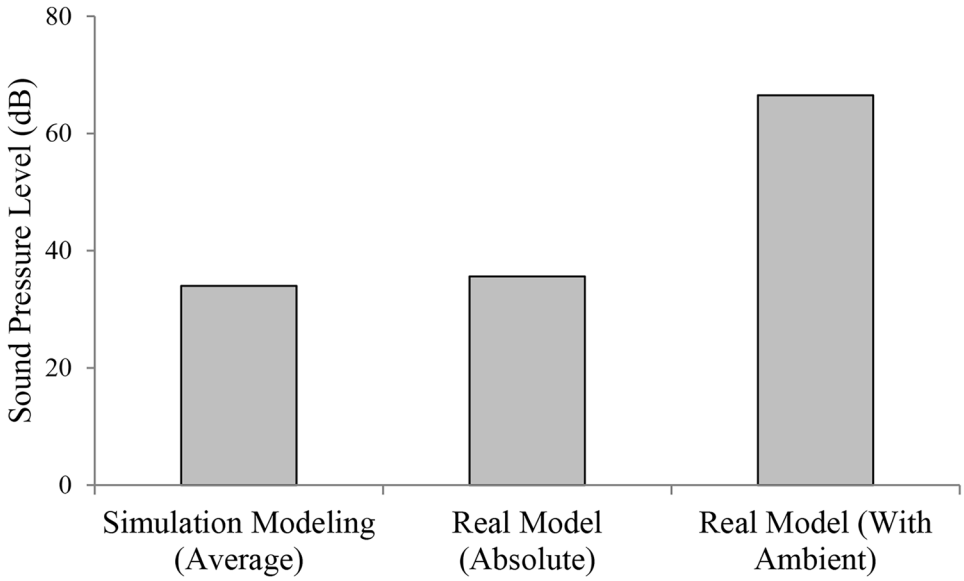

Fig. 4 Comparison of sound pressure levels in three different modes

environment, because high-speed imaging can determine the formation of cavitation phenomenon and the growth of cavitation clouds (Gavaises et al., 2015).

However, as mentioned, the scaling method was used to improve the image contrast and increase the pixel intensity. Considering that the effective coefficients can be obtained by trial and error (Giachetti & Asuni, 2011), in this section, a coefficient of 2 was selected to scale the images. In Fig. 5, the elapsed times are displayed in the first column, and the other columns are the images extracted from different color channels. According to this figure, the right column shows the status of paint dispersion as control, i.e., the glass bottle that was not treated with the ultrasonic transducer is shown. As seen, in this case after 60 s (1 min), the waterproof paint on the bottom of the glass bottle does not disperse, and only the paint on the top of the bottle moves down. By using RGB color channels, the image features can be extracted (Eyarkai Nambi et al., 2016). As can be seen in this figure, and comparing the images of different color channels at 10, 40, and 60 s (0.16, 0.66, and 1 min), it is observed that the images of the red color channel are clearer than the other channels and also more consistent with the RGB image.

Since the images extracted from red channel were more consistent with the RGB images, the histogram of this channel

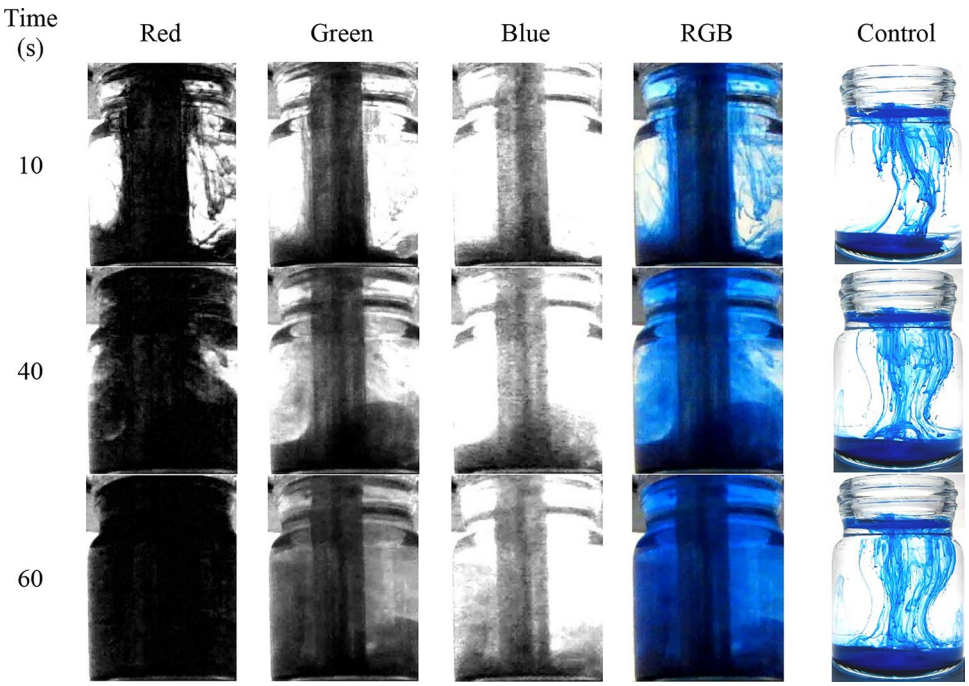

Fig. 5 Color images of the paint dispersion evolution, extracted from different color channels

was drawn for different elapsed times as shown in Fig. 6. At 10 and 20 s (0.16, and 0.33 min) elapsed times, which are shown in Fig. 6a and b respectively, it is observed that the higher gray scales have a small number of pixels, and the lower gray scales have less than 400 pixels, implying less dispersion of the paint. But over time at 40, 50, and 60 s (0.66, 0.83, and 1 min), which are shown in Figs. 6d, e and 5f, respectively, it is observed that the number of pixels with higher gray scales has decreased to zero, but the number of pixels with lower gray scales increased to values above 1000. The evolution of pixel's grayscale over time shows the paint dispersion process. This indicates that turbulence has occurred in the liquid due to the operation of the magnetostrictive ultrasonic transducer, which has caused the paint to spread.

For further investigation and eliminating the color effects of the transducer probe in the achieved images, the space around the transducer probe was divided into six parts, because depending on the type of research, parts of the image that are fixed or variable can be cut and deleted or processed (Labrosse et al., 2005). In other words, according to Fig. 7, three parts on the right side and three parts on the left side of the transducer probe with the same dimensions (60 pixels wide by 50 high) were selected. The red channel histograms data were extracted at 60 s (1 min), and the mean value was calculated for all gray scales. By analyzing this data, it was found that the mean value (72) is related to the gray scale 41. Therefore, to calculate the percentage of surface occupied by the waterproof paint in each of the six parts, all pixels whose gray scale was less than 73 were counted. Because by counting the number of pixels that have a special property, the amount of the surface and its changes can be achieved (Eyarkai Nambi et al., 2016). Then at different elapsed times, the number of pixels was introduced as a percentage of the occupied area. According to this figure, since the dispersion of waterproof paint at the bottom of the glass bottle is non-uniform, it is observed that the cropped image at the lower end of the left side has an occupancy level of 62% at 10 s (0.16 min), and at the end of 60 s (1 min) the occupied area reaches 81%. But at the lower right side, the occupied area is initially 28% and at the end about 100%. But in the middle parts, the paint dispersion speed increases from 20 to 40 s (0.33 to 0.66 min), so that in 40 s (0.66 min), more than 80% of these areas are occupied by blue paint. At the upper parts, up to 40 s (0.66 min), the dispersion speed is very low (less than 40%), but it is observed that between 40 and 60 s (0.66 to 1 min), this increases rapidly so that more

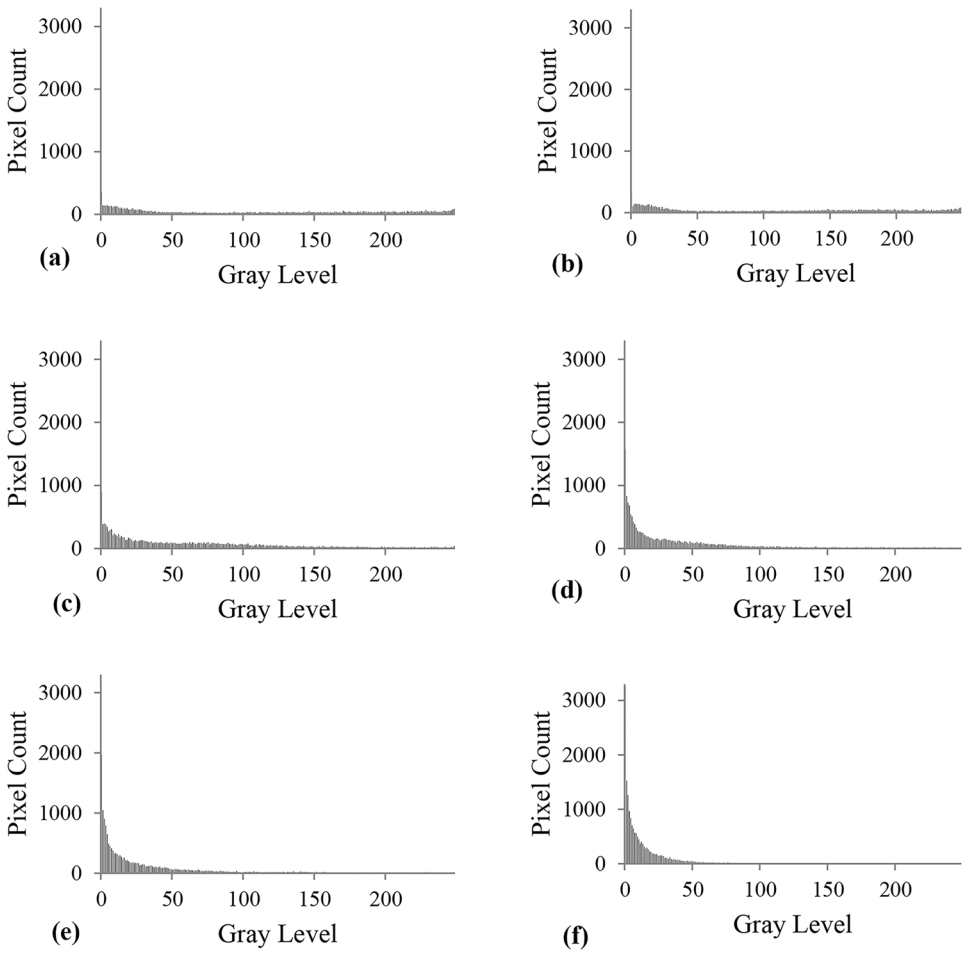

Fig. 6 Red channel histogram at different elapsed times of applying the paint. (**a**) 10 s. (0.16 min). (**b**) 20 s (0.33 min). (**c**) 30 s (0.5 min). (**d**) 40 s (0.66 min). (**e**) 50 s (0.83 min). (**f**) 60 s (1 min)

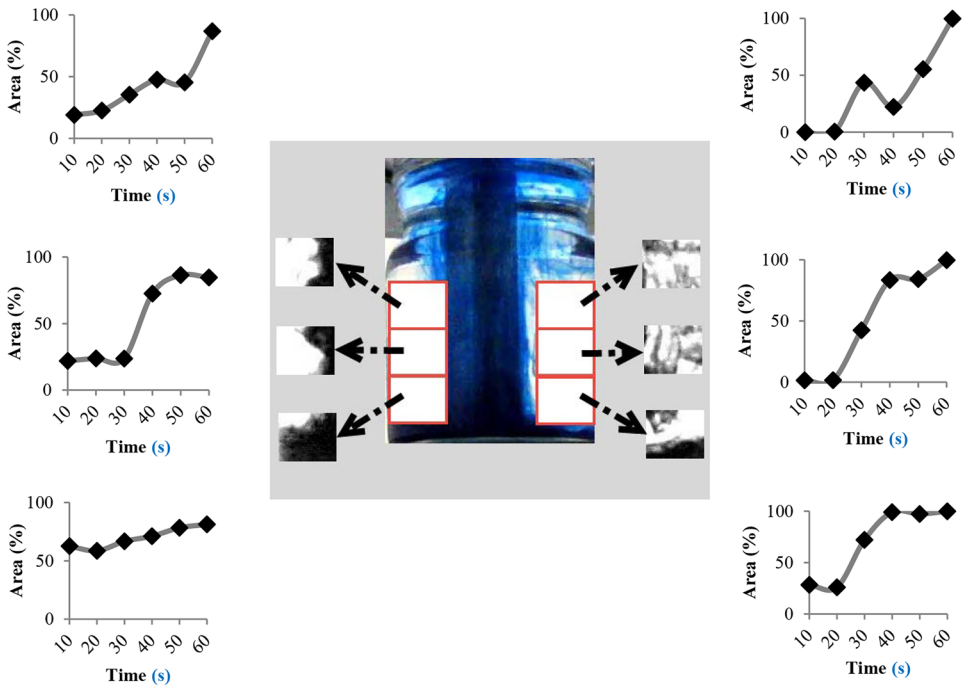

Fig. 7 Cropping the areas around the magnetostrictive ultrasonic probe into six parts with the same dimensions (60 pixels wide by 50 high). The location of the graphs correspond to the position of the cropped area

than 90% of these areas are occupied by blue paint. In other words, the cavitation phenomenon created by mechanical waves of the ultrasonic transducer initially creates bubbles at the lower parts. But over time, these bubbles burst and move upward to dissolve the blue paint in the middle and then the upper layers. Because over time and increasing the radius of the bubbles and reaching their critical radius and pressure, the bubbles become unstable and their density decreases, so the bubbles begin to move upwards. Also, by increasing the Reynolds number, which indicates turbulence in the fluid, tails are created on the new bubbles, which intensifies the cavitation phenomenon and increases the tendency to last longer after the disappearance of the main bubbles (Brennen, 2013). As a result, the magnetostrictive ultrasonic transducer causes the complete dispersion of the blue paint in the glass bottle for 60 s (1 min) by creating the cavitation phenomenon. In general, employing image processing method is useful in studying the dynamic behavior of clouds created by cavitation phenomenon in aqueous solvents (Hutli et al., 2019). So that by using gray images, dimensional parameters such as the length of the created cavitation clouds can be measured (Wu et al., 2019).

GC Test

Microorganisms are among the natural contaminants of fresh products. Observance of hygienic principles of such products is done by washing in tap water to remove residual pesticides, contaminants, and plant residues and reduce the microbial load on the peel of fruits (Fava et al., 2011). The effects of ultrasonic cleaning for 5, 10, and 20 min on the residual pesticide are shown in Table 3. Ultrasonic waves in water cause cavitation. Therefore, in the medium, micron-sized bubbles are formed quickly and burst. In such conditions, small explosions are created that provide the power of cleaning. According to this table, the Diazinon residue decreases with increasing time. Ultrasonic cleaning in 20 min has significantly reduced this pesticide. In other words, by using external standard method in GC test, the results showed that the residual pesticide based on the height of the chromatogram for the reference, 5, 10, and 20 min were 1, 0.27, 0.26, and 0.25, respectively. Also, the residual pesticide based on the area under the chromatogram for the reference, 5, 10, and 20 min were 1, 0.21, 0.18, and 0.17, respectively. In other words, using the magnetostrictive ultrasonic transducer for 20 min, the residual pesticide based on the height and chromatogram area were 25% and 17%, respectively. For ultrasonic cleaning, it is assumed that the sound bubbles created by the cavitation phenomenon oscillate over the peel products at a distance of several tens of nanometers. The flow created by the bursting of the bubble can lead to tensile and shear forces over the peel. This flow will cause cleaning (Lee et al., 2018). In a study that used ultrasonic treatment for 20 min to remove pesticides from cucumber product, the residual pesticides for trichlorfon, dimethoate, dichlorvos, fenitrothion, and chlorpyrifos were reported 17.1%, 47.8%, 50.2%, 15.6%, and, 37%, respectively (Liang et al., 2012). Also, in another study that used piezoelectric transducers with variable powers and times for tomato product, the results showed that by considering 300 W and 15 min, the residual pesticide for DDVP was 89% (Heshmati & Nazemi, 2018). Probably, the small volume of the lab beaker and also considering the 2

Table 3 GC test results for different treatment times on cucumber

Sample	Elapsed Time (min)	HBR*	Reduction (%)	ABR**	Reduction (%)
Reference	-	1	-	1	-
No. 1	5	0.27	73	0.21	79
No. 2	10	0.26	74	0.18	82
No. 3	20	0.25	75	0.17	83

*Height-based results

**Area-based results

min interval for each 1min treatment are the main reasons that have improved the results of this study compared to other studies. Because according to Table 3, by applying ultrasonic waves for 5 min, the reduction of Diazinon pesticide was more than 73%. On the other hand, in the ultrasonic bath, the power level is not high enough because the transducer vibrations enter the tank through a metal wall. Therefore, sound waves form a sustainable wave pattern in the tank, and the distribution of the ultrasonic field is not uniform. But the uniformity of this distribution in a probe system is less than in an ultrasonic bath. So that intense vibrations occur at the tip of the probe, causing a hole or corrosion in the metal probe (Lee et al., 2018).

SEM Imaging

The micro-images of the middle part of the cucumber were selected for measuring the dimensions of the peel features. All SEM images were taken at 2500 magnification and working distance of 8 mm. According to Fig. 8, the peel features of the cucumber product such as stomatal pores were observed by SEM images. In other words, the stomatal pores and their guard cells that are elliptic were evaluated. Stomatal pores are involved in the gas exchange of many fruits and vegetables such as cucumber and are embedded in the epidermis for several microns (Smith & Fleming,

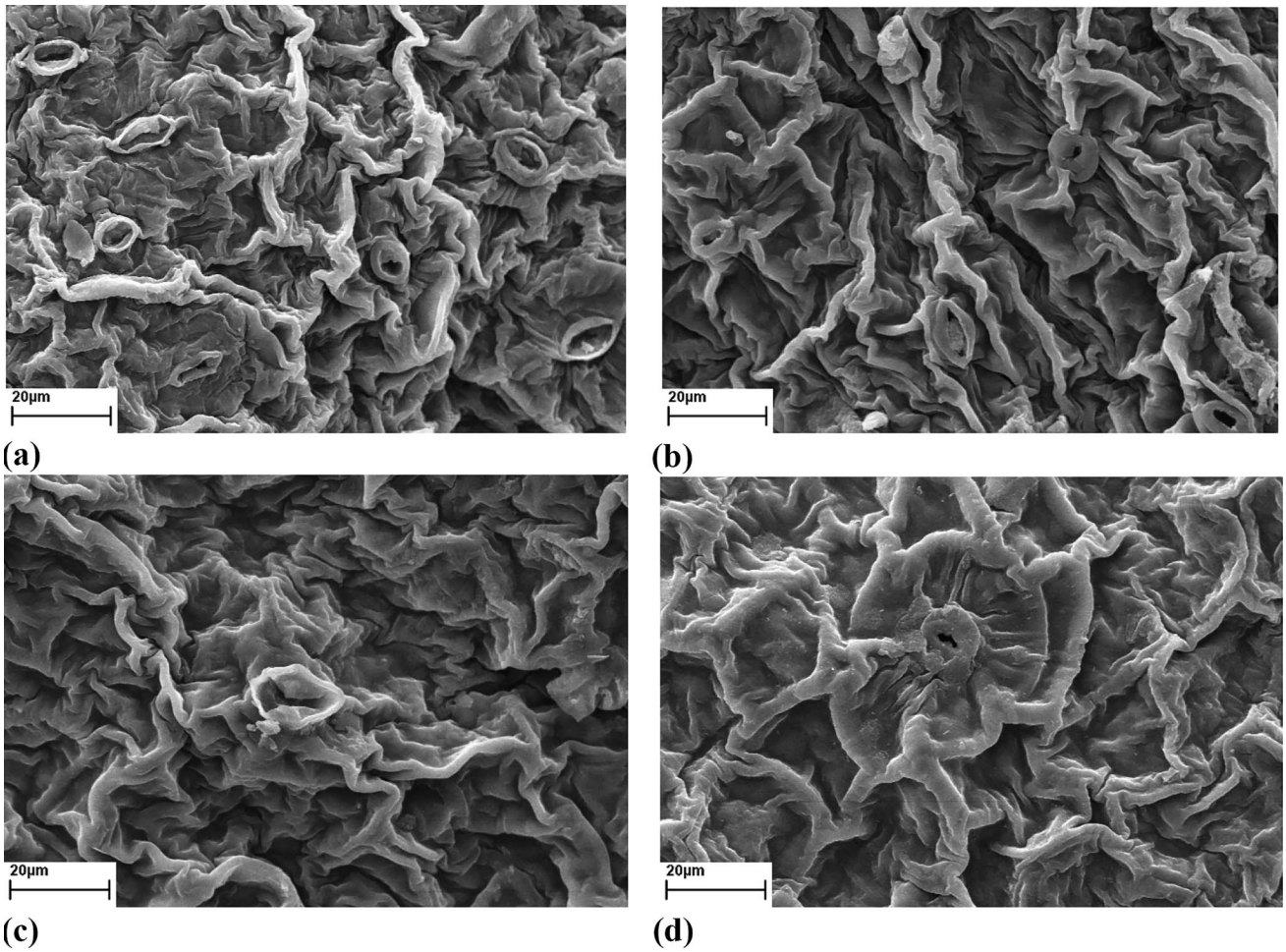

Fig. 8 SEM images for different treatment times. (**a**) Reference. (**b**) 5 min. (**c**) 10 min. (**d**) 20 min at 8 mm working distance, 20 kV voltage, and 2500 magnification

1979). As can be seen in this figure, by increasing the time of ultrasonic treatment, the opening area of stomatal pores decreases so that the highest opening area is related to the reference (Fig. 8a) and the lowest opening area is related to the 20 min treatment (Fig. 8d). The results of a study showed that by applying ultrasound for 2 min on the surface of the recalcitrant squash cotyledon, the stomatal pores and ridges of the guard cells were still in place. But after 10 min, the edges of the guard cells and the surrounding areas were smoothed. After 30 min, severe peel damage was observed so that epidermal cells and stomatal pores were damaged, and also large cracks were observed on the peel surface (Ananthakrishnan et al., 2007). As mentioned, ultrasonic waves not only clean the cucumber product, but also close the stomatal pores, and this will probably increase the shelf life of the product without affecting the content of organic and mineral materials as well as mechanical properties. Because according to the researches, the ultrasonic treatment of cherry tomatoes, strawberries, and palm fruits has almost doubled the shelf life without affecting their contents (Montalvo-González et al., 2018).

Also, according to Fig. 8, it is observed that with increasing treatment time, the peel texture of the cucumber product has been worn. So that by increasing this time, the depth of cavities on the cucumber peel has decreased and the pitting wall thickness has increased. The color uniformity in the 20 min treatment (Fig. 8d) compared to the 5 min treatment (Fig. 8b) justifies this peel erosion. The results of a study showed that by applying ultrasound for 2 min on the surface of the recalcitrant squash cotyledon, the surface of the epidermal cell in the reference was higher than the cell junctions. By applying ultrasonic treatment for 2 min, the surface of the epidermal cell and the cell junctions were disproportionately worn. By increasing the treatment time for 10 min, this erosion increased so that the surface of the epidermal cell was approximately equal to the cell junctions (Ananthakrishnan et al., 2007).

Ultrasound produces intense pressure, shear force, and temperature gradient in the material, which cause mechanical rupture in the texture. In other words, by propagation sound energy, which is mechanical oscillations, through the medium, three types of waves are created, which are (1) longitudinal waves that move in the direction of displacement, (2) shear waves that are perpendicular to the wave main motion, and (3) Rayleigh waves that travel very close to the material surface. Therefore, these three types of waves create alternating expansions and contractions. During these cycles, millions of small bubbles form that grow by absorbing energy from the medium, and when they cannot absorb more energy, they become unstable and burst violently. This releases a large amount of energy known as cavitation. A bubble can burst at or near the top of a cell wall. When this happens above the cell surface, it can potentially cause cavities in the cell wall (Montalvo-González et al., 2018). On the other hand, the bursting of bubbles created by transient cavitation causes serious physical conditions. These conditions include high temperature (up to 5000 K), high pressure (up to 1000 atm), high rate of cooling and heating (up to 1010 K/s), shock waveforms, and high-speed water jet (156 km/h) (Lee et al., 2018).

Photoshop software was used to investigate the effects of ultrasonic mechanical waves on the peel texture of cucumber products accurately. In other words, the dimensions of the stomatal pores, the guard cell wall thickness, and pitting wall

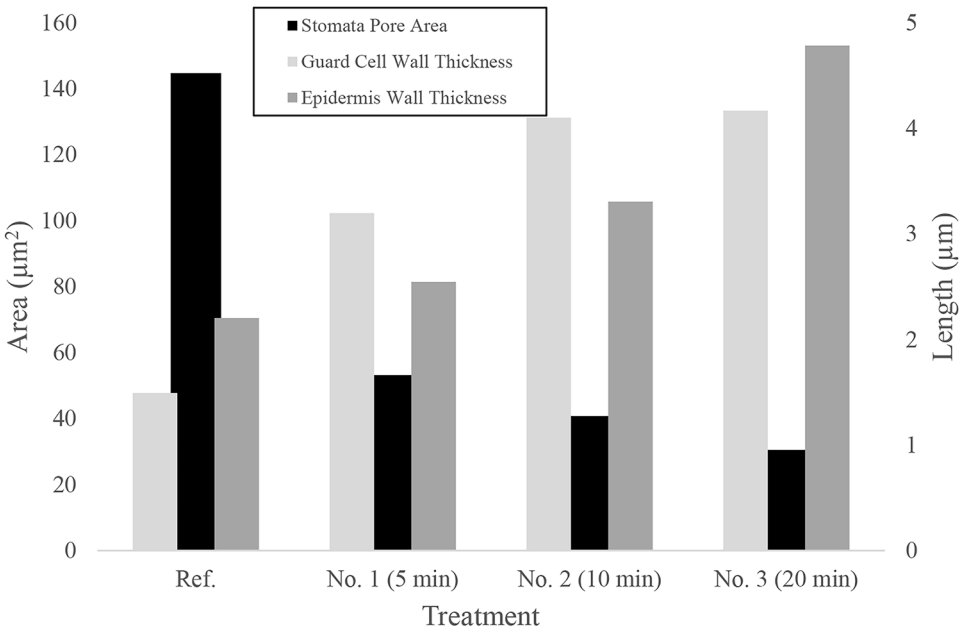

Fig. 9 Changes in stomatal pore area, guard cell wall thickness, and epidermis wall thickness for reference, 5-, 10-, and 20 min treatment times

thickness were calculated using the scaling method. Since the stomatal pores are ellipsoid, the area of these pores can be calculated using the ellipsoid area equation ($A = \pi ab$; where in this equation, A, a, and b are the stomatal pore area, the major diameter of the ellipse, and the minor diameter of the ellipse (Smith & Fleming, 1979)). Based on the effects of the cavitation phenomenon and what was mentioned above, according to Fig. 9 by increasing the treatment time, the stomatal pore area reduced from 144.74 μm^2 (reference) to 30.56 μm^2 (20 min treatment). Also, the guard cell wall thickness increased from 1.49 µm (reference) to 4.16 µm. But according to this figure, the increasing trend of guard cell wall thickness is ascendant for 10 min and then is almost constant. This trend may be due to the higher location of guard cells relative to the epidermis and also the lower thickness of the guard cell walls relative to the wall thickness of the epidermis cells. This increases the erosion process speed in the early minutes. Then the guard cell wall thickness increases due to erosion, and the cell height becomes equal to epidermis cells and as a result, the increasing trend of the guard cell wall thickness or erosion speed decreases. In addition, the epidermis wall thickness increased from 2.20 µm (reference) to 4.78 µm (20 min treatment). According to this figure, the increasing trend of the epidermis cell wall thickness is still ascendant. Therefore, by increasing ultrasonic treatment time, significant peeling will be done in the cucumber samples.

Conclusion

In this research, a magnetostrictive ultrasonic transducer was built, and its ability in creating cavitation in fluid (for cleaning of delicate fruits and vegetables) due to its generated mechanical waves was evaluated. Based on the previous finding, a conical core made of pure nickel (as an abundantly available, less expensive, less hazardous material) with a cone angle of 30° was used. The results showed that the sound pressure of the simulated model and the real transducer are almost the same. In addition, the ability of the transducer to disperse waterproof paints in aqueous solvent was evaluated by image processing method. Comparing the red, green, and blue channels with the RGB image, it was observed that the red channel is able to display more details of the RGB image. The results showed that the transducer is able to disperse more than 90% of waterproof paints in the glass bottle after 60 s (1 min). It was also observed that the cavitation phenomenon initially moves the paint at the bottom of the glass bottle and then causes to spread the paint towards the middle layers and finally in the upper layers. In addition, the GC test results showed that the residual pesticide based on the height and chromatogram area were 75% and 83%, respectively. Also, by increasing the treatment time, the stomatal pore area decreases so that the maximum opening area was observed in the reference and the minimum area for the sample of 20 min treatment time. By increasing the treatment time, the peel texture of cucumber is worn so that the epidermis cell depth decreased and the epidermis wall thickness. This erosion can be justified by comparing the color uniformity in the 20 min treatment and the 5 min treatment. However, as mentioned, one of the challenges of this study is the low effect of magnetostrictive nickel core. So a small lab beaker (250 ml) was selected to place two cucumbers with the ultrasonic horn. For future research, it is suggested that the effects of increasing the number of transducers and increasing the horn length in large container be investigated.

Acknowledgements The authors acknowledge technical support provided by the Ferdowsi University of Mashhad, Iran for this project.

Author Contribution Dr. Danial Gandomzadeh and Mrs. Yeganeh Sabeghi conceived the presented idea. Dr. Abbas Rohani and Mr. Soheil Movahed Fakhr developed the theory and performed the computations. Prof. Mohammad Hossein Abbaspour-Fard verified the analytical methods. All authors discussed the results and contributed to the final manuscript.

Funding This study was funded by Ferdowsi University of Mashhad (FUM), (grant number 46420).

Data Availability All data generated or analyzed during this study are included in this published article. Also, more information is available from the corresponding author on request.

Declarations

Competing Interests The authors declare no competing interests.

References

Ananthakrishnan, G., Xia, X., Amutha, S., Singer, S., Muruganantham, M., Yablonsky, S., Fischer, E., & Gaba, V. (2007). Ultrasonic treatment stimulates multiple shoot regeneration and explant enlargement in recalcitrant squash cotyledon explants in vitro. *Plant Cell Reports, 26*(3), 267–276. https://doi.org/10.1007/s00299-006-0235-1

Apostoaia, C. M. (2013). AC machines and drives simulation platform. *International Electric Machines & Drives Conference, 2013*, 1295–1299. https://doi.org/10.1109/IEMDC.2013.6556308

Azam, S. M. R., Ma, H., Xu, B., Devi, S., Siddique, M. A. B., Stanley, S. L., Bhandari, B., & Zhu, J. (2020). Efficacy of ultrasound treatment in the removal of pesticide residues from fresh vegetables: A review. *Trends in Food Science & Technology, 97*, 417–432. https://doi.org/10.1016/J.TIFS.2020.01.028

AZoM. (2004). *Stainless Steel - Grade 316L (UNS S31603)*. AZO Materials. https://www.azom.com/article.aspx?ArticleID=2382

Bartoli, M., Noferi, N., Reatti, A., & Kazimierczuk, M. K. (1996). Modeling Litz-wire winding losses in high-frequency power inductors. *PESC Record - IEEE Annual Power Electronics Specialists Conference, 2*, 1690–1696. https://doi.org/10.1109/PESC.1996.548808

Brennen, C. E. (2013). *Cavitation and bubble dynamics*. Cambridge University Press. https://doi.org/10.1017/CBO9781107338760

Cai, W., Feng, P., Zhang, J., Wu, Z., & Yu, D. (2016). Effect of temperature on the performance of a giant magnetostrictive ultrasonic transducer. *JVE Journals*, *18*(2), 1307–1318. https://jvejournals.com/article/16341

Cengiz, M. F., Certel, M., & Göçmen, H. (2006). Residue contents of DDVP (Dichlorvos) and diazinon applied on cucumbers grown in greenhouses and their reduction by duration of a pre-harvest interval and post-harvest culinary applications. *Food Chemistry, 98*(1), 127–135. https://doi.org/10.1016/j.foodchem.2005.05.064

Chang, C., Firouzi, K., Kyu Park, K., Sarioglu, A. F., Nikoozadeh, A., Yoon, H. S., Vaithilingam, S., Carver, T., & Khuri-Yakub, B. T. (2014). Acoustic lens for capacitive micromachined ultrasonic transducers. *Journal of Micromechanics and Microengineering, 24*(8), 085007. https://doi.org/10.1088/0960-1317/24/8/085007

Char, C. D., Mitilinaki, E., Guerrero, S. N., & Alzamora, S. M. (2010). Use of high-intensity ultrasound and UV-C light to inactivate some microorganisms in fruit juices. *Food and Bioprocess Technology 2010 3:6*, *3*(6), 797–803. https://doi.org/10.1007/S11947-009-0307-7

Cruz, R. M. S., Vieira, M. C., Fonseca, S. C., & Silva, C. L. M. (2009). Impact of thermal blanching and thermosonication treatments on watercress (Nasturtium officinale) Quality: Thermosonication process optimisation and microstructure evaluation. *Food and Bioprocess Technology 2009 4:7*, *4*(7), 1197–1204. https://doi.org/10.1007/S11947-009-0220-0

Doménech, E., Botella, S., Ferrús, M. A., & Escriche, I. (2013). The role of the consumer in the reduction of Listeria monocytogenes in lettuces by washing at home. *Food Control, 29*(1), 98–102. https://doi.org/10.1016/j.foodcont.2012.05.074

Eyarkai Nambi, V., Thangavel, K., Shahir, S., & Thirupathi, V. (2016). Comparison of various RGB image features for nondestructive prediction of ripening quality of "alphonso" mangoes for easy adoptability in machine vision applications: A multivariate approach. *Journal of Food Quality, 39*(6), 816–825. https://doi.org/10.1111/jfq.12245

Fang, S., Zhang, Q., Zhao, H., Yu, J., & Chu, Y. (2018). The design of rare-earth giant magnetostrictive ultrasonic transducer and experimental study on its application of ultrasonic surface strengthening. *Micromachines, 9*(3), 98. https://doi.org/10.3390/mi9030098

Fava, J., Hodara, K., Nieto, A., Guerrero, S., Alzamora, S. M., & Castro, M. A. (2011). Structure (micro, ultra, nano), color and mechanical properties of Vitis labrusca L. (grape berry) fruits treated by hydrogen peroxide, UV-C irradiation and ultrasound. *Food Research International*, *44*(9), 2938–2948. https://doi.org/10.1016/j.foodres.2011.06.053

Ferrentino, G., Komes, D., & Spilimbergo, S. (2015). High-power ultrasound assisted high-pressure carbon dioxide pasteurization of fresh-cut coconut: A microbial and physicochemical study. *Food and Bioprocess Technology, 8*(12), 2368–2382. https://doi.org/10.1007/S11947-015-1582-0

Gandomzadeh, D., & Abbaspour-Fard, M. H. (2020). Numerical study of the effect of core geometry on the performance of a magnetostrictive transducer. *Journal of Magnetism and Magnetic Materials, 513*, 166823. https://doi.org/10.1016/j.jmmm.2020.166823

Gandomzadeh, D., Abbaspour-Fard, M. H., Rohani, A., & Sharifi, M. (2022). The influence of coil parameters and core lamination factor on the performance of an ultrasonic transducer with a tapered core. *International Journal of Numerical Modelling: Electronic Networks, Devices and Fields, 35*(6), e3017. https://doi.org/10.1002/JNM.3017

Gavaises, M., Villa, F., Koukouvinis, P., Marengo, M., & Franc, J. P. (2015). Visualisation and les simulation of cavitation cloud formation and collapse in an axisymmetric geometry. *International Journal of Multiphase Flow, 68*, 14–26. https://doi.org/10.1016/j.ijmultiphaseflow.2014.09.008

Giachetti, A., & Asuni, N. (2011). Real-time artifact-free image upscaling. *IEEE Transactions on Image Processing, 20*(10), 2760–2768. https://doi.org/10.1109/TIP.2011.2136352

Gómez-López, V. M., Gil, M. I., Allende, A., Blancke, J., Schouteten, L., & Selma, M. V. (2014). Disinfection capacity of high-power ultrasound against E. coli O157:H7 in process water of the fresh-cut industry. *Food and Bioprocess Technology 2014 7:12*, *7*(12), 3390–3397. https://doi.org/10.1007/S11947-014-1346-2

Grange, A., & Brown, B. (1969). An investigation into the performance of nickel alloy magnetostrictive transducers prepared for commercial use - 1. *Applied Acoustics, 2*(2), 111–120. https://doi.org/10.1016/0003-682X(69)90013-9

Haughton, P. N., Lyng, J. G., Morgan, D. J., Cronin, D. A., Noci, F., Fanning, S., & Whyte, P. (2010). An evaluation of the potential of high-intensity ultrasound for improving the microbial safety of poultry. *Food and Bioprocess Technology*, *5*(3), 992–998. https://doi.org/10.1007/S11947-010-0372-Y

Heshmati, A., & Nazemi, F. (2018). Dichlorvos (Ddvp) residue removal from tomato by washing with tap and ozone water, a commercial detergent solution and ultrasonic cleaner. *Food Science and Technology, 38*(3), 441–446. https://doi.org/10.1590/1678-457x.07617

Hutli, E., Nedeljkovic, M., & Bonyár, A. (2019). Dynamic behaviour of cavitation clouds: Visualization and statistical analysis. *Journal of the Brazilian Society of Mechanical Sciences and Engineering, 41*(7), 1–15. https://doi.org/10.1007/s40430-019-1777-9

Ignat, A., Manzocco, L., Bartolomeoli, I., Maifreni, M., & Nicoli, M. C. (2015). Minimization of water consumption in fresh-cut salad washing by UV-C light. *Food Control, 50*, 491–496. https://doi.org/10.1016/j.foodcont.2014.09.036

Ishiyama, T., Kanai, Y., Ohwaki, J., & Mino, M. (2003). Impact of a wireless power transmission system using an ultrasonic air transducer for low-power mobile applications. *Proceedings of the IEEE Ultrasonics Symposium, 2*, 1368–1371. https://doi.org/10.1109/ultsym.2003.1293157

Smithells, C. J. (1976). *Metals Reference Book - 5th Edition*. Butterworth–Heinemann. https://www.elsevier.com/books/metals-reference-book/smithells/978-0-408-70627-8

Jiang, L., Gu, K., Liu, R., Jin, S., Wang, H., & Pan, C. (2019). Rapid detection of pesticide residues in fruits by surface-enhanced Raman scattering based on modified QuEChERS pretreatment method with portable Raman instrument. *SN Applied Sciences*, *1*(6). https://doi.org/10.1007/s42452-019-0619-9

Koesukwiwat, U., Lehotay, S. J., Miao, S., & Leepipatpiboon, N. (2010). High throughput analysis of 150 pesticides in fruits and vegetables using QuEChERS and low-pressure gas chromatography-time-of-flight mass spectrometry. *Journal of Chromatography A, 1217*(43), 6692–6703. https://doi.org/10.1016/j.chroma.2010.05.012

Labrosse, A., Woodland, A., & Labrosse, F. (2005). On the separation of luminance from colour in images. In *core.ac.uk*. http://users.aber.ac.uk/ffl/

Lafarga, T., Ruiz-Aguirre, I., Abadias, M., Viñas, I., Bobo, G., & Aguiló-Aguayo, I. (2018). Effect of thermosonication on the bioaccessibility of antioxidant compounds and the microbiological, physicochemical, and nutritional quality of an anthocyanin-enriched tomato juice. *Food and Bioprocess Technology*, *12*(1), 147–157. https://doi.org/10.1007/S11947-018-2191-5

Lee, H., Zhou, B., & Feng, H. (2018). Power ultrasound treatment of fruits and fruit products. In *Food Engineering Series* (pp. 311–333). Springer. https://doi.org/10.1007/978-1-4939-3311-2_11

Li, X., & Pan, Z. (2014). Dry Peeling of tomato by infrared radiative heating: Part II. Model validation and sensitivity analysis. *Food and Bioprocess Technology*, *7*(7), 2005–2013. https://doi.org/10.1007/s11947-013-1188-3

Liang, Y., Wang, W., Shen, Y., Liu, Y., & Liu, X. J. (2012). Effects of home preparation on organophosphorus pesticide residues in raw cucumber. *Food Chemistry, 133*(3), 636–640. https://doi.org/10.1016/j.foodchem.2012.01.016

Łoza, A., Bull, D. R., Hill, P. R., & Achim, A. M. (2013). Automatic contrast enhancement of low-light images based on local statistics

of wavelet coefficients. *Digital Signal Processing: A Review Journal, 23*(6), 1856–1866. https://doi.org/10.1016/j.dsp.2013.06.002

Lozowicka, B., Jankowska, M., Hrynko, I., & Kaczynski, P. (2016). Removal of 16 pesticide residues from strawberries by washing with tap and ozone water, ultrasonic cleaning and boiling. *Environmental Monitoring and Assessment, 188*(1), 1–19. https://doi.org/10.1007/s10661-015-4850-6

Mac Loughlin, T. M., Peluso, M. L., Etchegoyen, M. A., Alonso, L. L., de Castro, M. C., Percudani, M. C., & Marino, D. J. G. (2018). Pesticide residues in fruits and vegetables of the argentine domestic market: Occurrence and quality. *Food Control, 93*, 129–138. https://doi.org/10.1016/j.foodcont.2018.05.041

Maffei, D. F., Alvarenga, V. O., & Sant'Ana, A. S., & Franco, B. D. G. M. (2016). Assessing the effect of washing practices employed in Brazilian processing plants on the quality of ready-to-eat vegetables. *LWT - Food Science and Technology, 69*, 474–481. https://doi.org/10.1016/j.lwt.2016.02.001

Montalvo-González, E., Anaya-Esparza, L. M., Abraham Domínguez-Avila, J., & González-Aguilar, G. A. (2018). Ultrasonic processing technology for postharvest disinfection. In *Postharvest Disinfection of Fruits and Vegetables,* (pp. 101–119). Elsevier. https://doi.org/10.1016/b978-0-12-812698-1.00005-4

Pan, Z., Li, X., Khir, R., El-Mashad, H. M., Atungulu, G. G., McHugh, T. H., & Delwiche, M. (2015). A pilot scale electrical infrared dry-peeling system for tomatoes: Design and performance evaluation. *Biosystems Engineering, 137*, 1–8. https://doi.org/10.1016/j.biosystemseng.2015.06.003

Pinheiro, J. C., Alegria, C. S. M., Abreu, M. M. M. N., Gonçalves, E. M., & Silva, C. L. M. (2016). Evaluation of alternative preservation treatments (water heat treatment, ultrasounds, thermosonication and UV-C radiation) to improve safety and quality of whole tomato. *Food and Bioprocess Technology 2016 9:6*, *9*(6), 924–935. https://doi.org/10.1007/S11947-016-1679-0

Smith, K., & Fleming, H. (1979). Scanning electron microscopy of the surface of pickling cucumber fruit. *Scanning electron microscopy of the surface of pickling cucumber fruit*. https://fbns.ncsu.edu/USDAARS/Acrobatpubs/P121-150/p140.pdf

Sun, Y., Tao, J., Guo, F., Wang, F., Dong, J., Jin, L., Li, S., & Huang, X. (2023). AZ31B magnesium alloy matching layer for Lens-focused piezoelectric transducer application. *Ultrasonics, 127*, 106844. https://doi.org/10.1016/J.ULTRAS.2022.106844

Tapia, M. R., Gutierrez-Pacheco, M. M., Vazquez-Armenta, F. J., González Aguilar, G. A., Ayala Zavala, J. F., Rahman, M. S., & Siddiqui, M. W. (2015). Washing, peeling and cutting of fresh-cut fruits and vegetables. In *Food Engineering Series* (pp. 57–78). Springer. https://doi.org/10.1007/978-3-319-10677-9_4

Thomas, G. P. L., Chapelon, J. Y., Bera, J. C., & Lafon, C. (2018). Parametric shape optimization of lens-focused piezoelectric ultrasound transducers. *IEEE Transactions on Ultrasonics, Ferroelectrics, and Frequency Control, 65*(5), 844–850. https://doi.org/10.1109/TUFFC.2018.2817927

Tourkhani, F., & Viarouge, P. (2001). Accurate analytical model of winding losses in round Litz wire windings. *IEEE Transactions on Magnetics, 37*(1), 538–543. https://doi.org/10.1109/20.914375

Walkling-Ribeiro, M., Noci, F., Riener, J., Cronin, D. A., Lyng, J. G., & Morgan, D. J. (2008). The impact of thermosonication and pulsed electric fields on staphylococcus aureus inactivation and selected quality parameters in orange juice. *Food and Bioprocess Technology 2007 2:4*, *2*(4), 422–430. https://doi.org/10.1007/S11947-007-0045-7

Wang, B., Venkitasamy, C., Zhang, F., Zhao, L., Khir, R., & Pan, Z. (2016). Feasibility of jujube peeling using novel infrared radiation heating technology. *LWT - Food Science and Technology, 69*, 458–467. https://doi.org/10.1016/j.lwt.2016.01.077

Wang, X., Wang, Y., Shi, X., Gao, L., & Li, P. (2021). A probabilistic multimodal optimization algorithm based on Buffon principle and Nyquist sampling theorem for noisy environment. *Applied Soft Computing, 104*, 107068. https://doi.org/10.1016/J.ASOC.2020.107068

Wang, Z., Zhu, W., Miao, J., Zhu, H., Chao, C., & Tan, O. K. (2006). Micromachined thick film piezoelectric ultrasonic transducer array. *Sensors and Actuators, A: Physical*, *130–131*(SPEC. ISS.), 485–490. https://doi.org/10.1016/j.sna.2005.10.054

Wu, Q., Wei, W., Deng, B., Jiang, P., Li, D., Zhang, M., & Fang, Z. (2019). Dynamic characteristics of the cavitation clouds of submerged Helmholtz self-sustained oscillation jets from high-speed photography. *Journal of Mechanical Science and Technology, 33*(2), 621–630. https://doi.org/10.1007/s12206-019-0117-4

Wu, S., Nie, Y., Zhao, J., Fan, B., Huang, X., Li, X., Sheng, J., Meng, D., Ding, Y., & Tang, X. (2017). The synergistic effects of low-concentration acidic electrolyzed water and ultrasound on the storage quality of fresh-sliced button mushrooms. *Food and Bioprocess Technology*, *11*(2), 314–323. https://doi.org/10.1007/S11947-017-2012-2

Wygant, I. O., Kupnik, M., Windsor, J. C., Wright, W. M., Wochner, M. S., Yaralioglu, G. G., Hamilton, M. F., & Khuri-Yakub, B. T. (2009). 50 kHz capacitive micromachined ultrasonic transducers for generation of highly directional sound with parametric arrays. *IEEE Transactions on Ultrasonics, Ferroelectrics, and Frequency Control, 56*(1), 193–203. https://doi.org/10.1109/TUFFC.2009.1019

Xiu-ping, Z., Lin, M., Lan-qi, H., Jian-Bo, C., & Li, Z. (2017). The optimization and establishment of QuEChERS-UPLC–MS/MS method for simultaneously detecting various kinds of pesticides residues in fruits and vegetables. In *Journal of Chromatography B: Analytical Technologies in the Biomedical and Life Sciences,* (Vol. 1060, pp. 281–290). Elsevier B.V. https://doi.org/10.1016/j.jchromb.2017.06.008

Xu, W., & Wu, C. (2014). Decontamination of Salmonella enterica Typhimurium on green onions using a new formula of sanitizer washing and pulsed UV light (PL). *Food Research International, 62*, 280–285. https://doi.org/10.1016/j.foodres.2014.03.005

Zhang, L., Critzer, F., Davidson, P. M., & Zhong, Q. (2014). Formulating essential oil microemulsions as washing solutions for organic fresh produce production. *Food Chemistry, 165*, 113–118. https://doi.org/10.1016/j.foodchem.2014.05.115

Zudaire, L., Lafarga, T., Viñas, I., Abadias, M., Brunton, N., & Aguiló-Aguayo, I. (2018). Effect of ultrasound pre-treatment on the physical, microbiological, and antioxidant properties of calçots. *Food and Bioprocess Technology*, *12*(3), 387–394. https://doi.org/10.1007/S11947-018-2217-Z